Research Square

Preprints are preliminary reports that have not undergone peer review.
They should not be considered conclusive, used to inform clinical practice,
or referenced by the media as validated information.

The Effect of RF Magnetron Sputtered AlN Buffer in GaN Epitaxy by MOVPE on the m-plane Sapphire

Jiang Han
Tiangong University
Zhang Yi
BOE HC Semitek (Zhejiang) Co., Ltd.
Cheng Hu
BOE HC Semitek (Zhejiang) Co., Ltd.
Yuan Shuwei
BOE HC Semitek (Zhejiang) Co., Ltd.
Wang Wenjun
BOE HC Semitek (Zhejiang) Co., Ltd.
Niu Pingjuan
niupingjuan@tiangong.edu.cn
Tiangong University

Research Article

Keywords: sputtered AlN, semi-polar GaN, MOVPE

Posted Date: November 3rd, 2026

DOI: https://doi.org/10.21203/rs.3.rs-11206473/v1

License: This work is licensed under a Creative Commons Attribution 4.0 International License.
Read Full License

Additional Declarations: No competing interests reported.

Abstract

The GaN films deposited by metal organic vapor phase epitaxy (MOVPE) on m-plane sapphire using sputtered AlN as buffer with different oxygen and nitridation deposition conditions were studied. We find the suitable PVD condition that can be used for semi-polar GaN epitaxy. Only using nitridation for preparation and non-oxygen gas during deposition can result in a single crystal structure of semi-polar GaN. Further researches on the nitridation durations and film thicknesses have been discussed as well. By adjusting the nitridation and deposition durations appropriately, the photoluminescence (PL) intensities of GaN increased by 200% indicating the improvements of crystal qualities. The PVD AlN can replace the GaN buffer which may substantially reduce the epitaxy time and improve the crystalline quality of epi-layers.

1 Introduction

Since the high efficiency InGaN based LEDs were invented in 1990s, the metal organic vapor phase epitaxy (MOVPE) technology of GaN has been greatly developed[1–4]. Normally high-performance green or blue GaN/InGaN LED epi-layers are grown on the c-plane sapphire, which provides Ga-polar bulk structures with good crystal quality and features a smooth surface hardly corroded by chemicals. However, Ga-polar property also leads to strong intrinsic built-in electric fields causing the separations or less overlaps of electron and hole wave functions which is known as quantum confined Stark effect in InGaN/GaN or InGaN/AlGaN quantum wells (QCSE)[5–8]. The QCSE can significantly decrease the emitting efficiency and cause other problems such as the unconventional wavelength shift with the changing of the forward current.

In order to solve this problem, the researches on semi-polar and no-polar GaN epitaxy on either flat or patterned templates have been carried out for decades[9–14]. For the direction of built-in electric fields is not parallel to the applied electric fields, the QCSE can be greatly reduced. The polarity of GaN is determined by the growth plane of substrates and growth conditions (usually semi-polar GaN growth on the m-plane or the r-plane sapphire uses relatively thin AlN/AlGaN film or thick GaN film deposited in MOVPE chamber as buffer)[15–17]. However, the physical vapor deposition (PVD) AlN technology for Ga-polar GaN based LED with patterned sapphire substrate (PSS) has been widely applied in industrial production over these years. It can effectively improve the GaN epitaxial quality and reduce the manufacture time in great extent[18–20]. The GaN substrate can produce less dislocation density samples but the cost is much too high that it’s very difficult to be massively used[21, 22].

The nitridation of sputtered AlN is very different from the same name process in MOVPE. The former is achieved by RF alternating current (AC) field which is much weaker than the direct current (DC) field during sputtering[23–25]. The latter is achieved by ammonia pretreatment before VPE process[26]. Both of them can yield better crystal quality and higher electron mobility at proper conditions, indicating that there are some similar changes on substrate surface during the two different processes. The early research showed that the substrate surface became rougher and the surface density of nitride atoms

became larger with the nitridation time increasing[27]. For this reason, the nitridation process of sputtered AlN might determine or at least influence on the polarity of AlN and make AlN form into good shapes[28, 29]. However, the effect of oxygen added into sputtering reaction has not been fully understood. It was commonly considered as only being one of the transition factors from Al_2O_3 to AlN.

In this letter, we designed the AlN deposition condition with two variations——nitridation and oxygen, to study how PVD AlN affects the GaN growth on m-plane sapphire substrates.The thickness of AlN buffer is fixed on 33nm. The chemical depositions of GaN are done in one single process to ensure the sameness of growth conditions.

2 Experiment

The experiments were prepared using the 4-inches sapphire substrates with the thicknesses of 650±10μm. The four AlN templates on the m-plane sapphire substrates were deposited sequentially in the same PVD chamber using the same silicon carrier. The PVD equipment model is the Applied Endura Impulse produced by Applied Materials. The nitridation process before sputtering was achieved by using the RF electric field with 100W current power and the N_2 gas environment only. For the sputtering process, the main sputtering gases were Ar and N_2 and the ratio of flow rates kept 1:1. The oxygen flow rate was set as 5% of the argon. The deposition was achieved by using the 6kW DC power. To eliminate the batch-to-batch variations of the surfaces of the Al target, we introduced a stabilization step under the gas condition which would be used before starting the next run. The refractive index and thickness of AlN films shown in Table I were measured by the ellipsometer.

In the beginning we grew a sample with 150nm AlN buffer by MOVPE using pulse mode at 1150℃on the c-plane sapphire substrate and test it with XRD to make sure that the epitaxial recipe was effective. Then we repeated the process by replacing the AlN buffer of about 33nm by the sputtering PVD. The GaN growth last for 30 minutes at 1070℃, 75 torr. The GaN film thicknesses are about 2μm deduced from the reflectance curvatures monitored by MOVPE equipment.

At last, we made some other GaN samples on the m-plane sapphires with different nitridation times or AlN film thicknesses based on the optimized condition law we obtained from above and get their photoluminescence spectra with a 213nm laser.

3 Results and Discussion

3.1 Properties of AlN films

The thickness and refractive index status of AlN films tested by 633nm laser are shown in Table I. Each run contained two sapphires of m-plane and c-plane for comparison. The films on m-plane sapphire are about 8% thinner and the refractivities of the films are 0.06 ~ 0.07 larger than those on the c-plane sapphires. The result that refractive index decreases with more doped oxygen suggests the formation of

Al_2O_3 compound or crystal in AlN films for $n_{sapphire}<n_{AlN}$ confirmed by T. Hanada's study[23] on the PVD AlN films as well. The refractive indices of the films on the m-plane were 0.036 and 0.02 smaller in both with and without oxygen conditions respectively after adding the nitridation, while those of the films on the c-plane were only 0.013 and 0.006 smaller. The film thickness on the m-plane turned 0.58nm thicker with oxygen, while that on the c-plane turned 0.84nm thinner oppositely. The variations without oxygen are 1.78nm and 0.32nm thicker respectively. Even considering the experimental instabilities, it can still be concluded that the nitridation influence on the AlN films thicknesses on (10–10) is opposite to those on (0001), which might be caused by the very different internal stresses. The oxygen gas with nitridation seemed to be more influential. When the depositions were combined with the nitridation, the oxygen condition made the refractive indices 0.058 and 0.048 smaller on the m-plane and the c-plane, respectively. These differences turned to be 0.042 and 0.041 without the nitridation.

The growth direction of AlN on (10–10) of sapphire is not vertical to the substrate surface which might explain the differences of thicknesses between m-plane and c-plane. Considering the situation without oxygen or nitridation, the refractive index of the film on the m-plane is much bigger than that on the c-plane. First, we know the nucleation of AlN usually starts with anomalous islands or polycrystalline. The monomorph process can't be completed in such a small scale. Second, the bad crystal quality may lead to the anisotropy of refractive indices. According to Guenard's study[30], the c-plane Al_2O_3 surface is Al terminated. It can be easily deduced that the m-plane Al_2O_3 surface is either mix with the Al and O atoms or terminated by Al atoms as well but even rougher. These above factors may explain the differences between the phenomena on the m-plane and the c-plane.

The nitridation process shows some different influences especially with oxygen on the m-plane and the c-plane. It doesn't contain any oxygen gas during the process. Actually, it converted the Al-O into Al-N by constructing Al-N bonds directly or eliminating Al-O bonds in the first step. Both substances may have made the surfaces of m-plane and c-plane become more similar. Based on K. Uchida and C. Heinlein's study[26, 27], the nitridation affects the surface in the same way, no matter it is done by the RF plasma with the pure N_2 gas or by the MOVPE with the NH_3 gas. It produces a higher surface free energy which results in a completely Stranski-Krastanov growth mode. It seems that the nitridation make the oxygen dope into the AlN film more easily.

3.2 Properties of GaN Films

Figure 1 and Fig. 2 are the TEM images of the four samples on the m-plane. All the four samples were scanned by X-ray diffraction shown in Fig. 3.

The thicknesses of GaN in Fig. 1 are about 2.1μm in accord with the estimation from the reflectance curvatures. In this finite region, both of the GaN surfaces in Fig. 1(b) and Fig. 1(d) are rough. But their origins are different. Figure 1(b) contains a deep and huge pit. The dislocation lines under the pit coming from the bottom part are not so different from those of the other regions. The pit begins from the middle

of the GaN due to the bad crystal quality probably. The surface in Fig. 1(d) is uniformly rough because it's not c-plane.

The effect of nitridation process was estimated by comparing Fig. 1(a) to Fig. 1(c) and Fig. 1(b) to Fig. 1(d). The most significant differences are the obvious newly generated dislocation densities suddenly appearing in the middle of the GaN layers in Fig. 1(c). The GaN at the interface above the AlN shows typically features of the strain relaxation process—those cluttered and dense dislocation line. The wide screw dislocations gather into pipe-like structures extending to the surface. Most dislocations from the bottom are eliminated after about 800nm growth in Fig. 1(a), indicating that the relaxation process of the lattice can complete fast and fully when using the nitridation on the AlN films as preparation. Secondly, the dislocation lines in Fig. 1(d) are tilt, indicating the crystal orientation is not as same as Fig. 1(b). This will be confirmed by Fig. 3. However, the patterns formed by lines in the section of Fig. 1(b) & Fig. 1(d) seem to be similar to a certain extent. We supposed that the bottom GaN of Fig. 1(b) was same as that in Fig. 1(d), so the crystal orientation of GaN was determined by the condition of oxygen. To prove the hypothesis, we shall turn to Fig. 2, focusing on the interfaces between the GaN and the AlN.

Figure 2 shows the details of the interfaces between AlN buffers and GaN layers on the m-plane sapphires. The interfaces in Fig. 2(a) and (c) are both fuzzy while those in Fig. 2(b) and (d) are really sharp. Their conditions are divided by the existence of oxygen. Furthermore Fig. 2(a) and (c) both show the sharp bends or the step-like dislocation lines starting from about 30nm above the AlN buffers. This performance changes the crystal orientation from [0001] to [11–22]. It's hard to tell if the grey scale differences of GaN layers make sense. However, they indeed show some rules accompanied by the absence of oxygen as well. And the grey scales of AlN layers in the four images are almost the same which means the oxygen conditions of AlN layer resulted in the crystalline differences in either AlN or GaN.

It reveals that the GaN growth direction is tilted by approximately 0° relative to the substrate normal in Fig. 2(b) and 30° in Fig. 2(d), then turns to 0° and 23°within the first few nanometers in Fig. 1(b) and Fig. 1(d), indicating that the nitridation during AlN sputtering is critical for maintaining the semi-polar [11–22] growth. The TDD decreases significantly from ~ 8×10^{11} cm^{-2} near the AlN/GaN interface to ~ $3\times10^{10}cm^{-2}$ in the upper GaN layer. Furthermore, the interface RMS roughness is determined to be 1.84 nm, indicating a relatively abrupt interface. Under two-beam diffraction conditions, the dominant defects were identified as a-type edge dislocations, which are less detrimental to the optical properties of the semi-polar GaN. To confirm the crystal orientation of the GaN, we draw Fig. 3.

The ω-2θ scans on the four samples proves our guess on the effect of nitridation and oxygen on semi-polar GaN epitaxy straightly. All the samples' (30–30) peaks of m-plane sapphire had been corrected to the same degree. Only the sample on the AlN with nitridation but without oxygen shows intense signals of plane (11–22), while the samples on the AlN with oxygen show peaks of plane (0004). Combining the extremely flat surface, they are definitely Ga-face GaN. For the first purpose of this research is to find the

possibility of PVD AlN buffer used in semi-polar GaN epitaxy and the crystal quality should be bad without using the PSS to achieve the epitaxial lateral overgrowth (ELOG), the rocking curve results were above 1200 arcsecs. It should be noticed that the sample on the AlN without nitridation or oxygen shows some signals at about 33.7 degrees. We could not find the typical crystal orientation denoted by this peak. The peak intensity is always related to the layer thickness. We could infer that the characteristic peak was from the bottom GaN layers near the PVD AlN buffer. The bottom layers failed in forming semi-polar GaN without nitridation and the crystal lattice kept consistent with the sapphire. There are no other peaks except for the one from the sapphire, suggesting the GaN above is close to amorphous status.

Based on the results above, we adjusted the process durations by nitridation and deposition respectively (Table II) to get the optimizing directions. All the samples are made on the m-plane substrates and tested by the PL spectra afterward. All the dominant wavelengths were about 364nm in accord with the property of wurtzite GaN.

Figure 4(a) shows the PL results when the nitridation time changed from 20s to 120s with the deposition time being kept 60s. The intensity was enhanced with the increasing of nitridation time and was almost ten times enhanced comparing the result of 120s to that of 20s. The duration affects the nitridation area most. The peak wavelength changes from 363nm to 365nm as nitridation time increased from 20s to 120s, means the distances between atoms was turning bigger. Considering the sapphire gives compressive stress to the c-plane GaN during the epitaxy at all times, the enlargement of GaN lattice constant infers that the stress turns smaller. It supported that the nitridation is very important to the GaN nucleation on the m-plane sapphire substrate. It can compensate or be compensated by some other process parameters such as the AC power, the pressure, the temperature, etc.

Figure 4(b) shows the PL results when the deposition time changed from 30s to 150s with the nitridation time being kept 60s, meant the thickness of the AlN buffer changed from 21nm to 125nm according to the data of Table II. The growth rate turned fast with the depositing time increasing, suggesting that the surface energy turned larger and made the AlN synthesis more easily. The peak value of PL intensity increased three times from 30s to 120s, then decreased from 120s to 150s. The thickness of the AlN film affects most on the internal stress of the GaN which could change the curvature of template during the MOVPE process. The appropriate thickness of the AlN buffer is good for the distribution uniformity of the GaN. It can be adjusted with some other factors of MOVPE, such as the flow field affected by the pressure and the temperature, the growth rate and doping of GaN, etc. The peak wavelength changes from 363nm to 364nm with the deposition time increasing which meets expectations. Because the stress is released with the GaN turning thicker.

Finally, we summarized the results and provide our hypothesis on the semi-polar GaN formation process below. The nitridation improved the AlN surface energy and make the GaN grow in Volmer-Weber mode. This three-dimensional nucleation mechanism allows the crystallites to adjust their crystallographic orientation during the initial formation stage to release interfacial misfit stress. For m-plane sapphire, the (11–22) semi-polar plane may possess a lower effective nucleation barrier than the c-plane under such

high surface energy conditions, thereby being selectively favored. The surface arrangements of oxygen and nitrogen atoms on the m-plane sapphire exert different effects on inducing the polarity of GaN. Nitridation eliminates Al-O bonds and establishes Al-N bonds. This alteration in the chemical environment may modify the dipole moment at the interface, thereby inducing the GaN crystallites to tilt and transition from c-axis growth to inclined semi-polar growth. The growth direction of GaN is tilted by approximately 30° relative to the substrate (Fig. 2d). This tilting is the result of the crystal seeking its lowest energy configuration. During semi-polar growth, GaN accommodates the anisotropic stress of the m-plane sapphire substrate through inclined growth, utilizing internal basal plane stacking faults and prismatic plane dislocations. If the interface is too "perfect" or "sharp" (as in the case of oxygen incorporation), the crystal lattice becomes "locked" into a specific orientation, making it difficult to adjust to the semi-polar direction.

4 Conclusion

We prepared four GaN samples on m-plane sapphire using PVD AlN buffers. Our results indicate that excluding oxygen and adding nitridation are essential for achieving semi-polar [11–22] GaN nucleation, offering a viable path for mass production by addressing issues of crystal quality and time cost. While current crystalline quality requires optimization, the sputtered AlN buffer offers significant purity advantages over MOVPE. Future work should focus on optimizing deposition parameters and structural design, potentially extending these findings to N-face GaN epitaxy.

Declarations

Funding Declaration

This research did not receive any specific grant from funding agencies in the public, commercial, or not-for-profit sectors.

Author Contribution

Niu Pingjuan: conceptualizaition, supervision, resourcesJiang Han: conceptualization, methodology, validation, writing the original draft, writing-reviewing and editingZhang Yi: investigation, visualiazation on figure 1 and figure 2,writing the original draftCheng Hu& Yuan Shuwei: validation, data curation and vislualization on figure 3Wang Wenjun: validation, writing the original draftAll authors reviewed the manuscripit.

References

1. S. Nakamura, T. Mukai, M. Senoh, Appl. Phys. Lett. **64**, 1687–1689 (1994)
2. H. Amano, M. Kito, K. Hiramatsu, I. Akasaki, Jpn J. Appl. Phys. **28**, L2112 (1989)

3. I. Akasaki, H. Amano, Jpn J. Appl. Phys. **30**, L1705 (1991)
4. S. Pharkphoumy, V. Janardhanam, T.H. Jang et al., Electronics. **12**, 1049 (2023)
5. T. Takeuchi, S. Sota, M. Katsuragawa, M. Komori, H. Tekeuchi, H. Amano, I. Akasaki, Jpn J. Appl. Phys. **36**, L382 (1997)
6. T. Takeuchi, C. Wetzel, S. Yamaguchi, H. Sakai, H. Amano, I. Akasaki, Appl. Phys. Lett. **73**, 1691 (1998)
7. M. Leroux, N. Grandjean, M. Laügt, J. Massies, B. Gil, P. Lefebvre, P. Bigenwald, Phys. Rev. B **58**, R13371 (1998)
8. T. Deguchi, K. Sekiguchi, A. Nakamura, A. Nakamura, T. Sota, R. Matsuo, S. Chichibu, S. Nakamura, Jpn J. Appl. Phys. **38**, L914 (1999)
9. L. Jiu, Y. Gong, T. Wang, Sci. Rep. **8**, 1 (2018)
10. F. Scholz, Semi Sci. Tech. **27**, 024002 (2012)
11. D.F. Feezell, M.C. Schmidt, S.P. DenBaars, S. Nakamura, MRS Bull. **34**, 318 (2009)
12. A. Tyagi, H. Zhong, R.B. Chung, D.F. Feezell, M. Saito, K. Fujito, J.S. Speck, S.P. DenBarrs, S. Nakamura, Jpn J. Appl. Phys. **46**, L444 (2007)
13. Y. Enya, Y. Yoshizumi, T. Kyono, K. Akita, M. Ueno, M. Adachi, T. Sumitomo, S. Tokuyama, T. Ikegami, K. Katayama, Appl. Phys. Exp. **2**, 082101 (2009)
14. T. Kyono, Y. Yoshizumi, Y. Enya, M. Adachi, S. Tokuyama, M. Ueno, K. Katayama, T. Nakamura, Appl. Phys. Exp. **3**, 011003 (2010)
15. G. Zhao, L. Wang, S. Yang, H. Li, H. Wei, D. Han, Z. Wang, Sci. Rep. **6**, 1 (2016)
16. L. Zhou, R. Chandrasekaran, T.D. Moustakas, D. Smith, J. Crys Grow. **310**, 2981 (2008)
17. P. Vennéguès, T. Zhu, D. Martin, N. Grandjean, J. Appl. Phys. **108**, 113521 (2010)
18. C.H. Yen, W.C. Lai, Y.Y. Yang, T.K. Ko, S.J. Hon, S.J. Chang, IEEE Phot Tech. Lett. **24**, 294–296 (2011)
19. H. Wu, J. Ning, J. Zhang et al., Nanotechnology. **34**, 295202 (2023)
20. H. Hu, S. Zhou, H. Wan, X. Liu, N. Li, H. Xu, Sci. Rep. **9**, 1 (2019)
21. K. Iso, H. Yamada, H. Hirasawa, N. Fellow, M. Saito, K. Fujito, S.P. DenBaars, J.S. Speck, S. Nakamura, Jpn J. Appl. Phys. **46**, L960 (2007)
22. T. Nishida, H. Saito, N. Kobayashi, Appl. Phys. Lett. **79**, 711 (2001)
23. T. Hanada, M. Kobayashi, S. Tanabe, N. Soga, J. Non-cryst. Solids. **135**, 227 (1991)
24. Y. Cho, Y. Kim, E.R. Weber, J. Appl. Phys. **85**, 7909 (1999)
25. S.K. Kim, J.S. Yoo, J.M. Priest, M.P. Fewell, Surf. Coat. Tech. **163**, 380 (2003)
26. K. Uchida, A. Watanabe, F. Yano, M. Kouguchi, T. Tanaka, S. Minagawa, J. Appl. Phys. **79**, 3487 (1996)
27. C. Heinlein, J. Grepstad, T. Berge, H. Riechert, Appl. Phys. Lett. **71**, 341 (1997)
28. J.S. Paek, K.K. Kim, J.M. Lee, D.J. Kim, M.S. Yi, D.Y. Noh, H.G. Kim, S.J. Park, J. Crys Grow. **200**, 55 (1999)

29. A. Georgakilas, S. Mikroulis, V. Cimalla, M. Zervos, A. Kostopoulos, Ph. Komninou, Th. Kehagias, and Th. Karakostas, physica status solidi (a) 188, 567(2001)
30. P. Guenard, G. Renaud, A. Barbier, M. Gautier-Soyer, Surf. Rev. Lett. **5**, 321 (1998)

Tables

Table I. Each PVD process run contains one m-plane and one c-plane substrate for comparison. The AlN films on m-plane sapphires appear to be thinner and have high refractive index. The thickness and refractive index are measured by ellipsometry.

Type of substrate	Oxygen	Nitridation	Thickness (nm)	Refractive index
m-plane	yes	yes	32.98	2.003
c-plane			35.33	1.955
m-plane	no	yes	34.33	2.061
c-plane			36.10	2.003
m-plane	yes	no	32.40	2.039
c-plane			36.17	1.968
m-plane	no	no	32.55	2.081
c-plane			35.78	2.009

Table II. The combinations of nitridation times and deposition times using on the m-plane substrates. The growth rate of AlN increased with the deposition time.

Nitridation time	Depostion time	Thickness (nm)	Refractive index index
20s	60s	47.5nm	2.063
30s	60s	46.8nm	2.063
40s	60s	47.2nm	2.060
60s	60s	47.8nm	2.060
80s	60s	47.7nm	2.053
120s	60s	47.3nm	2.057
60s	30s	21.0nm	2.073
60s	120s	102.5nm	2.067
60s	150s	125.3nm	2.148

Figures

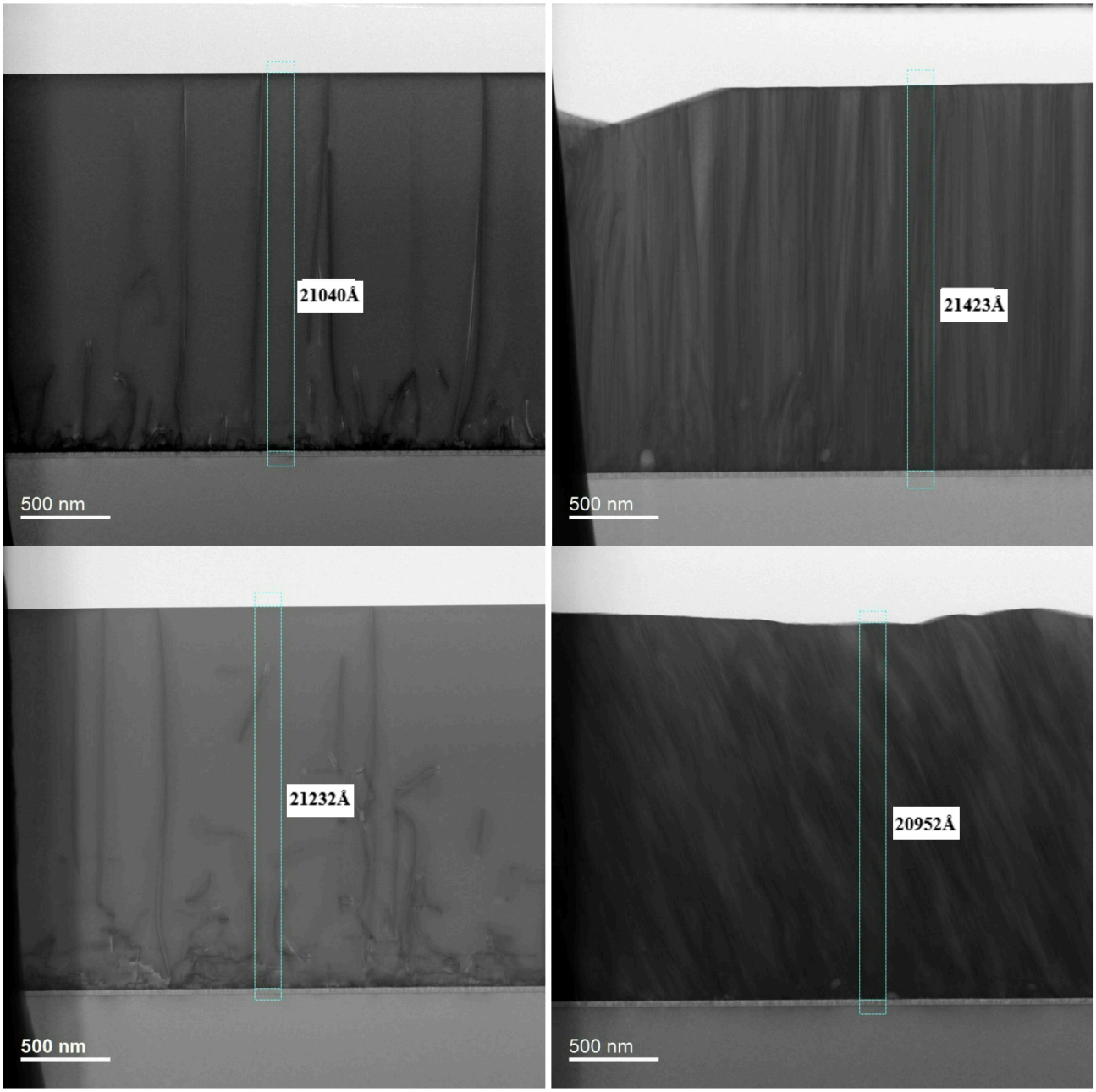


Figure 1

The TEM of GaN samples with the different sputtering AlN conditions on the m-plane sapphire.

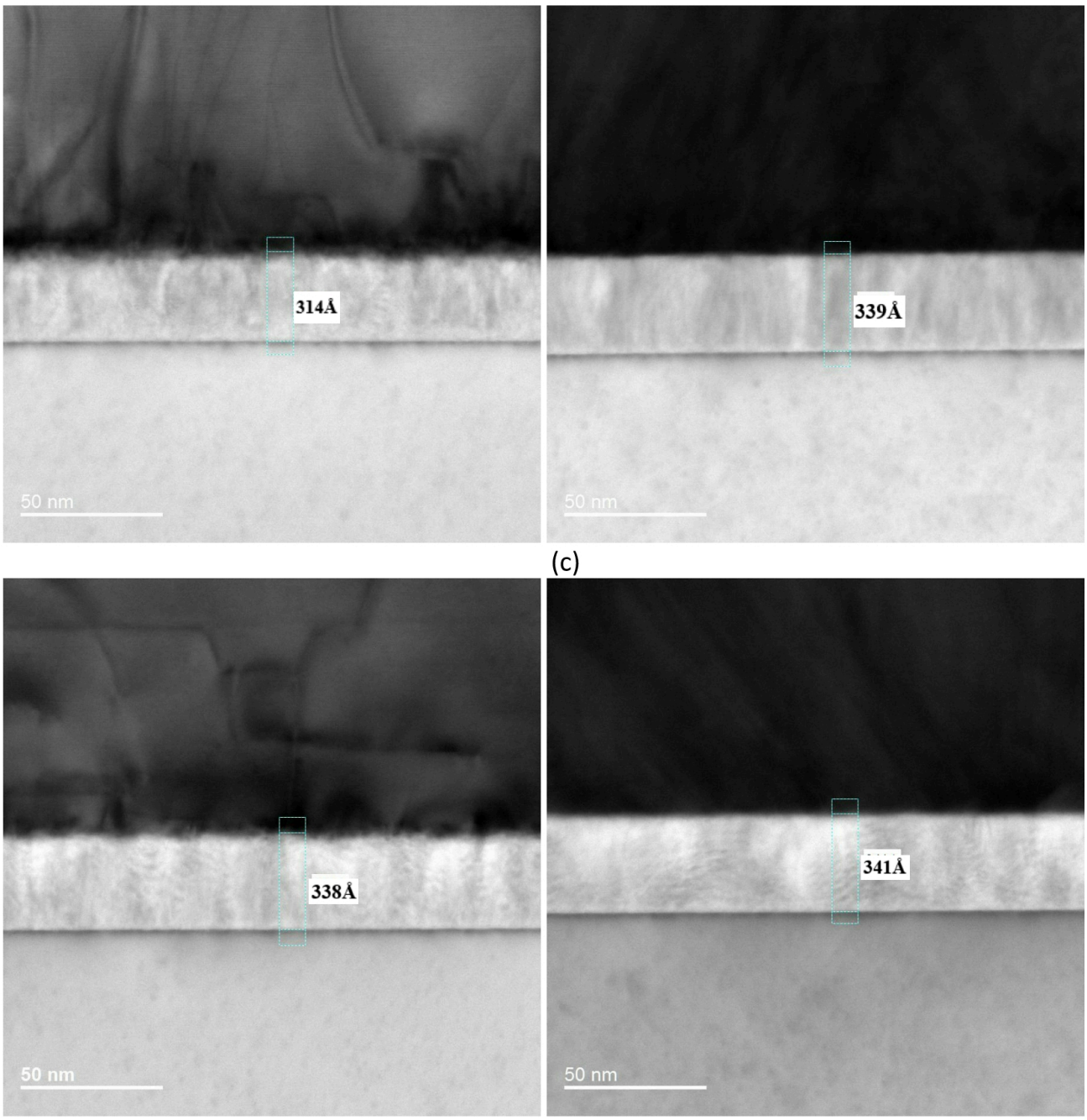


Figure 2

The interfaces between AlN buffers and GaN layers on m-plane substrates.

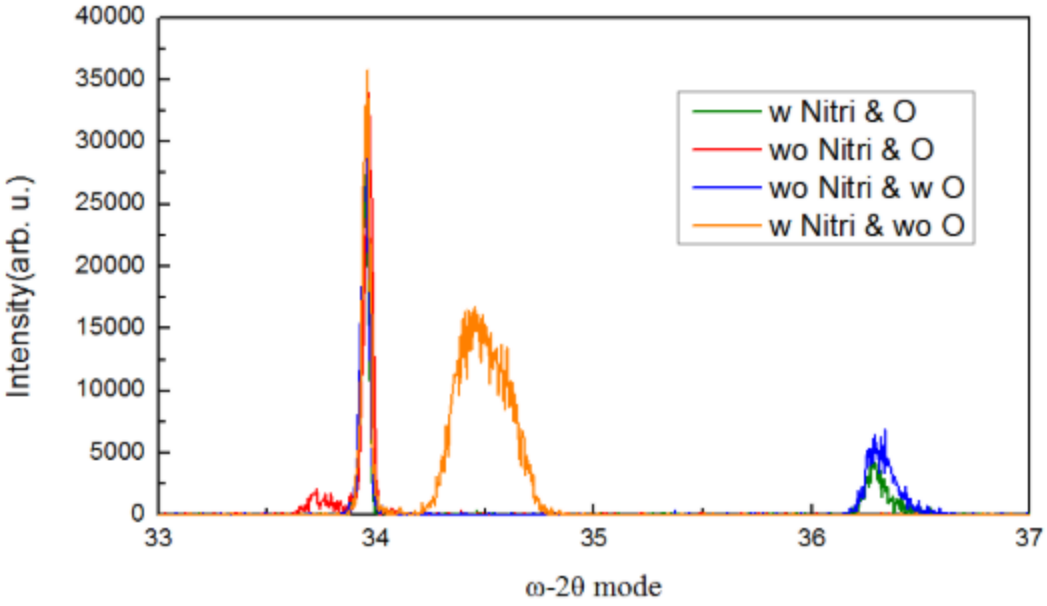


Figure 3

The XRD ω-2θ mode images of the 4 samples on m-plane sapphire distinguished by colors. Four specific peaks are detected. The (30-30) plane of Al_2O_3 peaks at the same angle position can be used for reference.

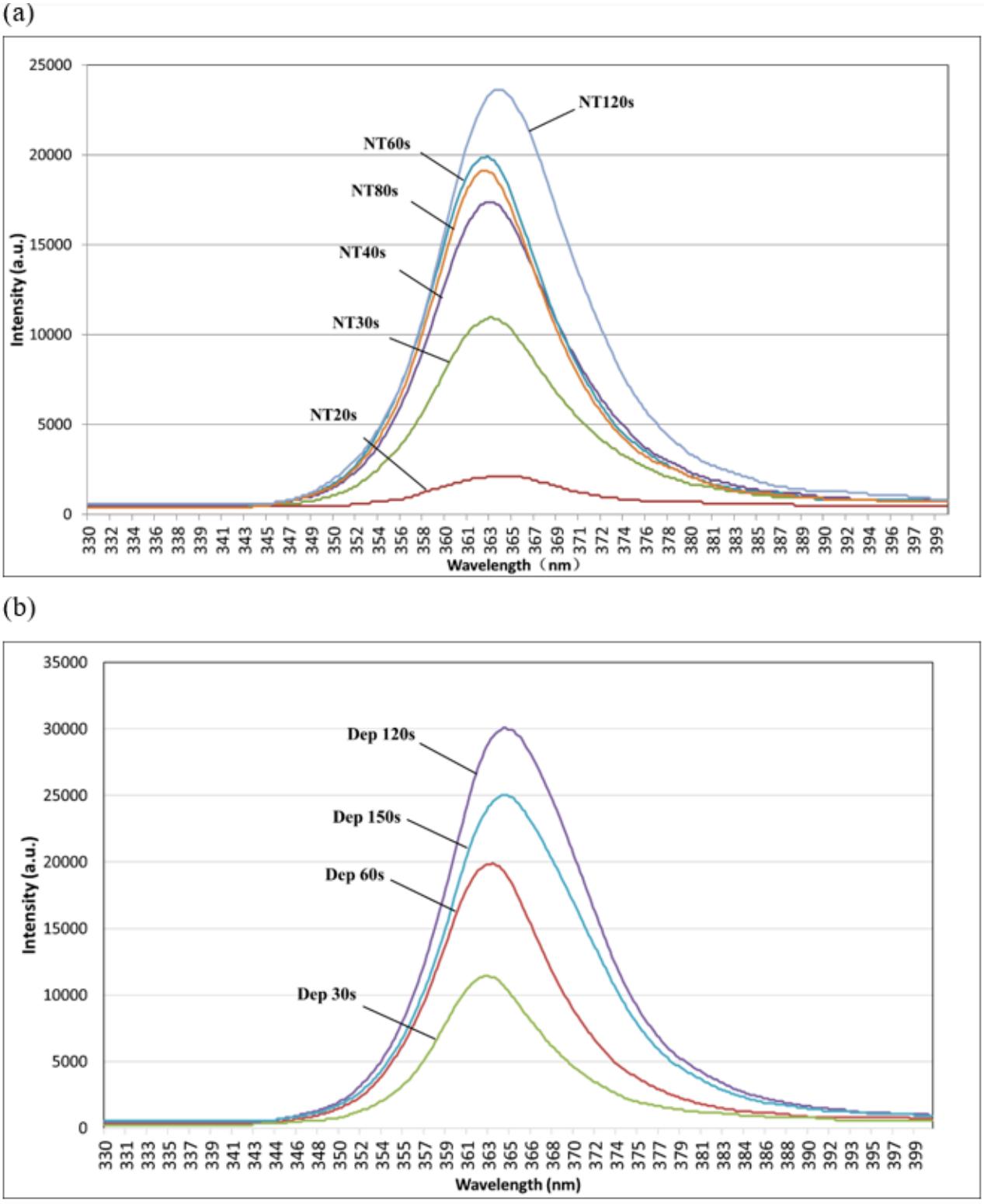


Figure 4

The PL spectra images of GaN samples grown on m-plane sapphire substrates with different AlN film buffers classified by (a) the different nitridation times (from 20s to 120s) with the same deposition time (60s) (b) the different deposition times (from 30s to 150s) with the same nitridation time (60s).